Intratumoral Recall of Childhood Vaccine-Specific CD4$^+$ T cells Coordinates Type I and II Antitumor Immunity

Authors: Michael C. Brown[1*], Zachary P. McKay[1], Yuanfan Yang[1], Georgia M. Beasley[2], David M. Ashley[1], Darell D. Bigner[1], Smita K. Nair[1,2], Matthias Gromeier[1*]

Affiliations:
[1]Department of Neurosurgery, Duke University Medical School, Durham, NC, USA
[2]Department of Surgery, Duke University Medical School, Durham, NC, USA

*Co-corresponding Authors:
Email: grome001@mc.duke.edu
Email: mcb52@duke.edu
Dept. of Neurosurgery
Duke University Medical Center, Box 3020
Durham, NC 27710

Author contributions: M.C.B., G.M.B., D.M.A., D.D.B., S.K.N., and M.G. contributed to study conception and design. M.C.B. and M.G. administered the project and carried out statistical analyses. M.C.B., Z.P.M., and Y.Y. performed experiments and acquired data; M.C.B. and M.G. wrote the manuscript and all authors participated in reviewing and editing.

Competing Interest Statement: M.C.B., D.M.A., D.D.B., S.K.N., and M.G. own intellectual property related to this research, which has been licensed to Istari Oncology, Inc. M.C.B, M.G., and D.D.B are paid consultants of Istari Oncology, Inc.; M.G. and D.D.B hold equity in Istari Oncology, Inc. S.K.N., M.C.B., D.D.B., and M.G. are inventors on patent application PCT/US2017/039953 held/submitted by Duke University that covers the composition and methods for activating antigen presenting cells with PVSRIPO. All other authors declare they have no competing interests.

Keywords: CD4$^+$ T cells, recall responses, eosinophils, ILC2s, poliovirus, tetanus, cancer immunotherapy
This PDF file includes:
Main Text
Figures 1 to 7

ABSTRACT

$CD4^+$ T cells are key contributors to cancer immune surveillance. Here we report that childhood vaccine associated antigens engage simultaneous antitumor functions of $CD8^+$ T cells and eosinophils via intratumor vaccine-specific $CD4^+$ T cell recall. Prior vaccination against poliovirus potentiates antitumor efficacy of polio virotherapy in mice, and intratumor recall of poliovirus or tetanus immunity delayed tumor growth. Antitumor effects of recall antigens were mediated by $CD4^+$ T cells, independent of CD40L signaling, and were dependent on eosinophils and $CD8^+$ T cells. Recall antigen therapy caused marked tumor infiltration of type 2 innate lymphoid cells (ILC2s) expressing granzyme B and PD1 and eosinophils, coinciding with decreased proportions of intratumor Tregs. A pan-cancer analysis revealed an inverse relationship between intratumor eosinophils and Tregs, but not $CD4^+$ or $CD8^+$ T cells. This work defines cancer immunotherapy potential of childhood vaccines and implicates type II immunity in $CD4^+$ T cell cancer immune surveillance.

INTRODUCTION

Adaptive immune memory rapidly engages anti-pathogen immunity upon repeat pathogen exposure/infection. Accordingly, recall responses, i.e. activation of adaptive memory cells upon encounter of their cognate antigen, orchestrate broad, localized innate and adaptive pro-inflammatory reactions capable of limiting replication of pathogens through antigen -dependent and -independent mechanisms[1,2]. Recent evidence implies cancer immunotherapy utility of recall responses: activating intratumor antiviral $CD8^+$ T cells was shown to mediate cancer immunotherapy[3], prior vaccination against Newcastle disease virus (NDV) potentiated the antitumor efficacy of NDV in mice[4], and Tetanus toxoid enhanced migration of dendritic cell vaccines[5].

It remains to be determined if $CD4^+$ T cell recall specific to routine vaccine antigens (e.g. Poliovirus or Tetanus toxoid) hold cancer immunotherapy potential, particularly those delivered in Th2 polarizing conditions (e.g. with alum adjuvant). Despite long-standing evidence that Th1-centric immunity is optimal to mediate effective cancer immunotherapy, Th2 polarized responses hold antitumor potential[6], associations between eosinophils and clinical cancer immunotherapy treatment are widely reported[7,8], and type II innate lymphoid cells (ILC2s) have been shown to contribute to the antitumor efficacy of PD1 blockade[9,10]. To date, much of the focus on engaging $CD4^+$ T cell help for cancer immunotherapy has been on antigen-specific cancer vaccines encompassing both MHC-II and MHC-I antigens using Th1 polarized immunization strategies[11].

PVSRIPO, the live-attenuated poliovirus (Sabin) type 1 vaccine modified with the internal ribosomal entry site (IRES) of human rhinovirus type 2[12], has shown early evidence of efficacy in recurrent glioblastoma[13] and recurrent, non-resectable melanoma[14] after intratumor administration.

Poliovirus, hereafter 'polio', vaccination is part of the standard pediatric immunization schedule worldwide, either with the live attenuated (Sabin), or the inactivated (Salk) vaccines. The coding sequence of PVSRIPO is identical to the type 1 Sabin vaccine. Pre-existing serum anti-polio (type 1) antibodies were confirmed in all patients receiving PVSRIPO therapy[13-15]. Moreover, clinical use of PVSRIPO entails prior boost with trivalent Salk (IPOL^{TM}) at least 1 week before intratumor PVSRIPO administration, which triggered increased serum anti-polio neutralizing antibody responses in all patients evaluated to date[13,14]. The antitumor efficacy of PVSRIPO requires viral replication in polio vaccine naïve mice[15,16], and encompasses both direct tumor cell killing and tumor-localized inflammation[15,17,18]. Thus, anti-polio immunological memory, which coincides with neutralizing antibodies, is likely to impede PVSRIPO replication within the tumor, but may provide an alternate antitumor mechanism of action through intratumor recall of T cells specific to polio vaccine antigens.

Using murine tumor models of melanoma and breast cancer, we demonstrate the inflammatory and antitumor potential of PVSRIPO therapy is bolstered by prior polio immunization in a $CD4^+$ T cell dependent manner, despite repression of intratumor virus replication. Triggering intratumor recall with polio and tetanus antigens induced marked $CD4^+$ T cell, type 2 innate lymphoid cell (ILC2), and eosinophil influx, and mediated antitumor efficacy through $CD8^+$ T cells and eosinophils in a CD40L independent manner.

RESULTS

Polio immunization potentiates polio virotherapy. We first tested seroconversion of mice transgenic for the human poliovirus receptor CD155 (hCD155-tg) upon immunization with trivalent Salk vaccine (IPOL™) or PVSRIPO (to mimic type 1 Sabin) with and without the Th2-promoting adjuvant alum (alhydrogel; ALH), part of licensed standard vaccine formulations (e.g. Pentacel®, Pediarix®, Kinrix®) that enhances Salk vaccine immunogenicity[19]. A duration of 45 days post initial immunization before tumor implantation ensured sufficient time for establishment of immunological memory[20]. IPOL™ alone achieved limited seroconversion, while PVSRIPO immunization elicited a stronger antibody response; ALH bolstered antibody responses to both vaccines (**Fig 1A, B**). To recapitulate the high levels of serum neutralizing anti-polio antibodies in cancer patients prior to PVSRIPO therapy [typically >1:10,000 plaque neutralization titers[13]], we chose PVSRIPO + ALH (hereafter 'polio') immunization to determine the role of pre-existing polio immunity in PVSRIPO immunotherapy. Murine tumor models expressing the human poliovirus receptor CD155 and hCD155-tg mice were previously developed to permit entry and replication of PVSRIPO in neoplastic and non-malignant cells of the tumor microenvironment, and PVSRIPO was adapted to murine neoplastic host cells (mRIPO) to mediate infection and lysis[17,21]. The antitumor efficacy of intratumor mRIPO was superior in polio immunized mice relative to control (keyhole limpet hemocyanin; KLH) immunized counterparts in melanoma (B16) and breast (E0771) cancer models (**Fig 1C, D**). Immunization with IPOL™ + ALH, generating lower anti-polio serum neutralizing antibody titers than PVSRIPO + ALH (**Fig 1A, B**), modestly enhanced antitumor effects of mRIPO therapy (**Fig S1**). Thus, prior immunization to polio bolsters the antitumor efficacy of polio virotherapy.

Polio virotherapy in polio vaccine naïve mice is associated with T cell inflammation within the tumor[15,17]. To determine how recall responses to polio antigens alter the tumor microenvironment (TME) after polio virotherapy we analyzed tumors at various intervals (**Fig 1E**). mRIPO replication within tumors was substantially reduced in polio immunized mice 2- and 5-days post-treatment (**Fig 1F**), consistent with high neutralizing antibody titers (**Fig 1B**). Increased total immune cell density ($CD45.2^+$ cells) in polio immunized mice 7 days after mRIPO therapy was observed, explained largely by an influx of eosinophils and conventional $CD4^+$ T cells, with reduced proportions of Tregs (**Fig 1G, H**). Neutrophil-, NK cell-, and B cell infiltration after mRIPO therapy was indistinguishable from controls (**Fig S2A**). These observations were reproducible in a separate tumor model, E0771, wherein $CD11b^+$, $Ly6G^{neg}$, $F480^+$, $SSC\text{-}A^{hi}$ cells (consistent with eosinophils) and conventional $CD4^+$ T cells explained the majority of tumor-infiltrating immune cells after mRIPO therapy in polio vaccinated mice (**Fig S2B, C**).

T cell functional phenotypes are augmented in polio immunized mice treated with mRIPO. $CD8^+$ and $CD4^+$ tumor-infiltrating lymphocytes (TILs) in polio vaccinated mice expressed higher levels of intracellular TNF at day 7-, and higher IFNγ, TNF, and Granzyme B at day 12 post-mRIPO treatment in the $B16^{hCD155}$-OVA model, implying enhanced functional status (**Fig 2A**). Notably, no difference in the frequency of CD44 expressing memory $CD4^+$ or $CD8^+$ T cells was observed (**Fig 2A**). TILs from polio immunized mice treated with mRIPO also exhibited increased differentiation phenotypes with expression of the transcription factors Tbet, GATA3, and RORγt; as well as induction of IRF4, a promoter of T cell activation and function (**Fig 2B**)[22]. Expression of the T cell exhaustion markers PD1 and TIM3 on tumor $CD4^+$ T cells in the tumor and TDLNs of polio vaccinated mice treated with mRIPO were reduced (**Fig S2D**). Changes in T cell

activation/differentiation markers were consistent in the E0771 orthotopic breast cancer model (**Fig S2E, F**). Collectively, these findings implicate the recall response to polio in potentiation of T cell function after intratumoral polio virotherapy.

Polio and tetanus recall antigens mediate antitumor efficacy. We hypothesized that immunological memory to polio antigen may potentiate polio virotherapy via antitumor effects of adaptive recall responses since viral replication—required for both viral-induced innate inflammation and oncolysis[15]— was dramatically reduced in polio immunized mice (**Fig 1F**). To probe the antitumor effects of polio antigen we used a model devoid of hCD155 (mice and tumors) and treated tumors with UV-inactivated PVSRIPO ('UVP') to preclude tumor cell/TME infection and viral replication. We included comparisons with another vaccine-associated recall antigen, Tetanus toxoid (Tet). Intratumor therapy with UVP exerted antitumor efficacy exclusively in polio immunized mice; Tet treatment mediated a transient antitumor effect only in Tet immunized mice (**Fig 3A, B; Fig S5**). We confirmed these effects in mice co-immunized with clinical grade Tenivac® (tetanus and diphtheria) and IPOL™: intratumor therapy with UVP and Tet mediated antitumor efficacy exclusively in Tenivac + IPOL™ immunized mice (**Fig 3C**). Natural recall responses typically occur in the presence of a localized innate immune response to pathogen replication. To mimic this, Tet or polio immunized mice were treated with high molecular weight poly(I:C) alone or in combination with UVP or Tet. Both UVP and Tet mediated pronounced antitumor effects in this context (**Fig 3D**). To gauge inflammatory potential of Polio and Tetanus antigens in humans, we measured cytokine responses to UVP, Tet, and IPOL™ relative to poly(I:C) (positive control) after 6 days (**Fig 3E**), wherein CXCR3 ligands (CXCL9, 10, 11), IFNs (IFNα/β/λ/γ), and other cytokines were induced. PBMCs from patients with recurrent GBM

mounted similar responses to UVP and Tet (**Fig 3F, Fig S5D-F**), indicating that immunological memory to tetanus and polio vaccines are not compromised in patients with heavily pre-treated, advanced cancer. Together, these observations indicate potential of recall antigens in inducing antitumor effects.

CD4$^+$ T cells mediate the antitumor efficacy of recall antigens. Our observations indicate antitumor potential of polio/tetanus antigens only after antigen-matched immunization; thus, the adaptive immune system must initiate the antitumor effects caused by 'recall' antigen. To determine which adaptive compartment(s) mediate(s) antitumor efficacy of recall responses, we compared intratumor treatment of UVP in CD8$^+$ T and B cell knockout (k/o) mice relative to wildtype (wt) mice (**Fig 4A**). We did not address this question in CD4 k/o mice due to the anticipated role of CD4$^+$ T cells in influencing both CD8$^+$ T cell and B cell responses to vaccination, rendering the comparison uninformative. Polio immunization in wt and CD8 k/o mice led to anti-polio antibody production; as expected, sera from polio immunized B cell k/o mice did not react to polio capsid (**Fig 4B**). B16 tumor growth was similar in each genetic context after mock treatment. Relative to wt mice, the antitumor efficacy of UVP in polio immunized mice was limited in CD8 k/o mice at later time points, and was enhanced in B cell k/o mice (**Fig 4C**). Eosinophils express Fcγ receptors, contribute to antibody dependent cellular cytotoxicity, and may be influenced by antibody/complement-mediated activites[23]. To test if eosinophil influx or other changes observed in the TME after polio recall (**Fig 1**) are dependent on B cells (or antibodies), we analyzed tumor infiltrating cells seven days after treatment in polio immunized wt vs B cells k/o mice after mock or UVP treatment. Similar to polio virotherapy in polio immunized mice, UVP treatment led to increased immune cell influx, eosinophil infiltration, along with increased

$CD4^+$ T cells—decreased proportions of which were Tregs (**Fig 4D**). Thus, the antitumor efficacy of polio recall is independent of, and possibly countered by, B cells, and partially dependent upon $CD8^+$ T cells. These observations, along with robust $CD4^+$ T cell infiltration in tumors after mRIPO therapy (**Fig 1G**), suggest that $CD4^+$ T cells dictate the antitumor efficacy of polio recall responses. To test if polio-specific $CD4^+$ T cell recall responses are sufficient to potentiate the antitumor efficacy of mRIPO therapy, we isolated $CD4^+$ T cells from polio or Tet immunized mice, transferred them to naïve recipients bearing B16 tumors, and treated tumors with DMEM (control) or mRIPO. The antitumor efficacy of mRIPO was markedly enhanced in mice with $CD4^+$ T cell adoptive transfer from polio immunized mice relative to that of Tet immunized mice (**Fig 4E**). We repeated this experiment comparing transfer of $CD4^+$ T cells from spleens of KLH vs. polio immunized mice (**Fig S6**). Similarly, the antitumor efficacy of mRIPO was enhanced after transfer of $CD4^+$ T cells from polio vaccinated mice. Thus, $CD4^+$ T cells mediate the antitumor efficacy of polio recall.

Intratumor recall antigen therapy potentiates antitumor $CD8^+$ T cell function. Tumor-specific $CD4^+$ T cells were shown to mediate antitumor efficacy through direct tumor cell killing[24-26], engagement of cytotoxic innate immune cells[27,28], or by providing $CD4^+$ T cell help to effector $CD8^+$ T cells[29-32]. Our data demonstrate that recall antigens not expressed by tumor cells (i.e. vaccine associated antigens), also engage antitumor functions of $CD4^+$ T cells when delivered intratumorally (**Figs 3-4**). The lack of expression and thus, MHC class II presentation, of recall antigens in cancer cells within this system precludes the contribution of direct antigen-specific cancer cell killing by cytolytic $CD4^+$ T cells. Rather, mRIPO therapy in polio vaccinated mice was associated with enhanced polyfunctional $CD8^+$ T cell phenotypes (**Fig 2**), and the antitumor effect of UVP in such mice was tempered in mice lacking $CD8^+$ T cells (**Fig 4C**). Thus, we next sought

to determine if polio (UVP) and Tet recall enhances the function of antitumor $CD8^+$ T cells. To this end we adoptively transferred $CD45.1^+$ marked, *ex vivo* SIINFEKL-stimulated OT-I $CD8^+$ T cells to polio or Tet vaccinated mice and determined the impact of UVP and Tet-induced recall on B16-OVA tumor infiltrating OT-I T cell phenotype (**Fig 5A**). As in prior studies, induction of recall responses in the tumor after UVP (in polio immunized mice) or Tet (in Tenivac immunized mice) was associated with delayed tumor growth and increased tumor infiltration of $CD45^+$ cells, eosinophils, and conventional $CD4^+$ T cells (**Fig 5B**). A non-significant, but consistent increase in OT-I and endogenous $CD8^+$ TILs was also observed (**Fig 5B**). Analysis of tumor infiltrating OT-I $CD8^+$ T cells revealed enhanced Granzyme B, TNF, and IFNγ after UVP treatment in polio immunized mice or Tet treatment in Tenivac immunized mice (**Fig 5C**). As observed in polio vaccinated mice after mRIPO therapy (**Fig 2B, D**), transcription factors associated with varied Th polarizations were induced in both OT-I and endogenous T cells, including GATA3, RORγT, and BCL6 (**Fig 5C**). To asses changes in antitumor T cells after intratumor polio recall in an unbiased manner, tumor infiltrating OT-I T cells were isolated after mock or UVP treatment of polio immunized mice and their transcriptomes were analyzed by RNA-sequencing (**Fig 5D, Fig S8**). Downregulated expression of genes associated with NF-κB and SRC signaling (*S100b, RSAD2, Mpzl1*) coincided with increased expression of granzymes; genes linked with T cell activation, function, or homeostatis (*Taok3, CD86, CCR5, Egr2, Adgre1, Vdr, IRF4,* and *BCL6*); genes associated with Th1 immunity (*Ptger4, Fgl2*); as well as genes associated with Th2 immunity (*Alox15, Ccl8,* and *GATA3*) (**Fig S8C**). Demonstrating enhanced immunological memory against B16-OVA tumors after intratumor recall, T cells isolated from spleens of mice in which intratumor recall occurred (UVP in polio vaccinated, or Tet in Tenivac vaccinated) delayed tumor growth upon transfer to mice implanted with B16-OVA tumors (**Fig 5E**). Collectively, these observations

indicate that intratumor recall antigen therapy potentiates the function of antitumor T cells with both Th1- and Th2-associated attributes.

Tumor infiltrating eosinophils inversely associate with Tregs in human tumors.

In addition to increased T cell functional phenotypes and $CD4^+$ T cell infiltration coinciding with reduced proportions of Tregs, polio and tetanus recall was associated with a marked increase in tumor infiltrating eosinophils (**Figs 2, 4 and 5**). Tumor eosinophil influx has been shown to be associated with immunotherapy response[7,8,10], eosinophils can contribute to immune surveillance[33], and vaccination with GMCSF expressing tumor cells contributed to antitumor effects of $CD4^+$ T cell help in an IL-5 dependent manner[34]. To query whether a natural relationship exists between eosinophils and the tumor immune microenvironment composition in human tumors, we analyzed a pan-cancer TCGA data set[35] for relationships between eosinophils and other immune cell types. Using previously computed CIBERSORT[36] prediction of cell infiltrates[35], samples from each cancer type were stratified by presence or absence of detected eosinophil gene expression signatures (**Fig 6A, Figs S9-10**); TGCT and UVM were excluded from downstream analyses due to limited numbers of cases with eosinophil enrichment ($n < 3$). Low grade gliomas (LGG) had the highest eosinophil enrichment across all tested tumor types, with most tumor types having between 5 - 20% of the cases with detected eosinophil signatures (**Fig S9A**). While no significant association of eosinophil presence was observed with $CD8^+$ or $CD4^+$ T cell enrichment, eosinophil presence was associated with significantly lower Treg, but increased monocyte signatures across all cancer types (**Fig 6A, Fig S9B-C**). The detection of eosinophils was associated with longer survival in LGG, but not other tumor types (**Fig 6B, Fig S9D**). Significant differences in Treg density upon stratification by eosinophil enrichment were observed within

several cancer types, with heterogenous relationships between $CD4^+$ and $CD8^+$ T cell density (**Fig S10A**). In melanoma (SKCM) and colon adenocarcinoma (COAD), eosinophil presence was associated with significant $CD4^+$ T cell enrichment (**Fig S10B**). These data may reflect a role for eosinophils in influencing tumor infiltrating T cell biology, in particular, Tregs.

Antitumor type II immunity after mRIPO treatment of polio immunized mice. Eosinophil recruitment can be mediated by innate lymphoid type 2 cells (ILC2s), which coordinate Th2 responses through direct interactions with $CD4^+$ T cells[37], express the transcription factor GATA3 and eosinophil recruiting cytokine IL-5, but lack T cell receptor expression. In gating from prior experiments originally designed to detect GATA3 expression in T cells (**Fig 5B-C**), we noted increased $GATA3^+$ $CD3^{Neg}$ cells in tumors of mice after triggering intratumor recall with either polio or tetanus antigen (**Fig 6C**), possibly reflecting ILC2 influx. We next tested how eosinophils impact PVSRIPO therapy in polio immunized mice, and measured ILC2s directly. Polio immunized, B16-OVA^{hCD155} tumor bearing mice with and without concomitant eosinophil depletion [via anti-IL-5 antibody[38]] were treated with mock or mRIPO (**Fig 6D, E**). Eosinophil depletion, which was confirmed in blood and tumors 14 days after treatment (**Fig 6F, Fig S11C**), mitigated the antitumor effects of polio recall (**Fig 6E**). Depletion of eosinophils did not reduce $CD4^+$ T cell influx after PVSRIPO treatment in polio immunized mice, but blocked reductions in Treg proportion (**Fig 6F**). Thus, eosinophils are associated with decreased Treg density in human tumors (**Fig 6A**), and suppress Treg populations during recall antigen therapy. Moreover, intratumor PVSRIPO therapy led to ILC2 influx (**Fig 6F**) and altered ILC2 phenotypes, with reduced IL-5 and induced PD1 and Granzyme B expression (**Fig 6G**). These data demonstrate antitumor roles for eosinophils and recruitment of ILC2s with altered phenotypes after recall

antigen therapy. Recent work indicated that PD1-expressing ILC2s contribute to immune checkpoint blockade therapy[9,10]. Possibly due in part to PD1-expressing ILC2s, recall antigens potentiated anti-PD1 therapy in mice (**Fig 6H**).

The antitumor efficacy of polio recall is independent of CD40L-CD40 signaling. A key mechanism by which $CD4^+$ T cell help mediates antitumor efficacy is through CD40L signaling to CD40 on antigen presenting cells[29]. Indeed, agonistic antibodies to CD40 are being tested as cancer immunotherapy agents[39]. To determine if recall antigens mediate antitumor effects through CD40 signaling, we compared the antitumor efficacy of polio recall with and without CD40L blockade (**Fig 7A, B**) in the context of OT-I $CD8^+$ T cell transfer as in Figure 5. While a trend towards more aggressive tumor growth was observed after CD40L blockade, it did not affect antitumor effects of UVP or UVP-elicited influx of ILC2s, eosinophils, conventional $CD4^+$ T cells, or antitumor OT-I T cells (**Fig 7B**). Moreover, an agonistic anti-CD40 antibody did not recapitulate ILC2 and eosinophil influx observed after recall antigen therapy, but was instead associated with an increase in tumor associated macrophage density (**Fig 7C, D**). Thus, we conclude that intratumor $CD4^+$ T cell recall engages antitumor type I and II immunity independent of CD40-CD40L signaling.

DISCUSSION

This work reveals cancer immunotherapy potential of triggering tumor-localized $CD4^+$ T cell recall responses. Intratumor polio recall responses culminated in multifaceted inflammatory responses encompassing both innate and T cell compartments in a $CD4^+$ T cell-dependent manner. $CD8^+$ T cells and eosinophils contributed to the antitumor efficacy of polio recall/PVSRIPO therapy in polio vaccinated mice, indicating that $CD4^+$ T cell recall engages multiple antitumor effectors.

$CD4^+$ T cell help is critical for generation of fully functional antitumor $CD8^+$ T cell responses[11,29] and the development of long-term memory $CD8^+$ T cells[31,40]. Antitumor $CD8^+$ T cells exhibited greater polyfunctional phenotypes after recall response induction, adoptive transfer of T cells from recall antigen treated mice delayed tumor growth in naïve recipients, and the antitumor effect of UVP was blunted in polio immunized mice lacking $CD8^+$ T cells. These findings indicate provision of $CD4^+$ T cell help to antitumor $CD8^+$ T cells during polio virotherapy and/or injection of polio/tetanus antigen into tumors. Indeed, $CD4^+$ T cell help is associated with downregulation of T cell exhaustion markers, increased TNF/IFNγ/Granzyme B expression in effector T cells, and induced Tbet and IRF4 expression in 'helped' effector T cells[30], all of which were observed after polio virotherapy in polio immunized mice in the current study. Such T cell help is likely mediated through multiple mechanisms, including enhanced activation of tumor antigen presenting dendritic cells; $CD4^+$ T cell secretion of $CD8^+$ T cell supportive cytokines/chemokines like IL-21 and IFNγ; reprogramming the TME to a $CD8^+$ T cell supportive environment, e.g. via IFNγ secretion to induce MHC-class I antigen presentation; or through recently described effects of eosinophils on $CD8^+$ T cell immune surveillance[33]. Retained antitumor efficacy of polio recall in the context of

CD40L blockade and the failure of CD40 agonism to recapitulate recall antigen therapy phenotypes indicate that the antitumor and inflammatory effects of recall antigens do not rely entirely on CD40L signaling.

The antitumor efficacy of polio recall responses only partially depended on $CD8^+$ T cells. Recall antigen therapy was associated with robust eosinophil and ILC2 influx, and depletion of eosinophils revealed their role in mediating antitumor effects in polio immunized mice treated with mRIPO. In asthma, $CD4^+$ T cells have been shown to recruit eosinophils[41], in a process mediated by ILC2s[42]. ILC2s express MHC-class II and interact with $CD4^+$ T cells to propagate Th2 responses in the context of helminth infection[37]. In cancer, tumor infiltration of eosinophils is linked with immunotherapy response in patients[7,8], eosinophils were shown to support $CD8^+$ T cell immune surveillance[33], and ILC2s express PD1 and contribute to the antitumor efficacy of PD1 blockade[9,10]. In the current study, we discovered an inverse relationship between tumor eosinophil influx and Treg density in human cancers, possibly reflecting a role for eosinophils in Treg suppression. Indeed, recall antigen therapy caused eosinophil influx, and was associated with decreased proportions of Tregs in a manner dependent upon eosinophils/IL-5. Prior work also points towards a relationship between Tregs and eosinsophils: depletion of Tregs led to increased eosinophil influx in murine tumor models[43], and decreased Treg proportions and function has been noted in asthmatic lung tissue[44], in which eosinophils commonly infiltrate. We also observed increased PD1 and Granzyme B expression in tumor-infiltrating ILC2s after polio recall, possibly indicating their transition to an antitumor phenotype amenable to PD1 blockade. Indeed, despite stagnant or even reduced expression of PD1 on T cells after recall antigen treatment, recall antigen therapy accentuated the antitumor efficacy of PD1 blockade. Varying ILC2 phenotype states have

been observed[45], including their transition to a "Th1-like" state[46,47]. Perhaps highlighting the importance of context, both eosinophils and ILC2s have also been shown to mediate pro-tumorigenic effects[48-50].

Notably, we used Th2 polarizing vaccination strategies, consistent with the clinical administration strategies of polio and tetanus vaccines, to demonstrate antitumor potential of $CD4^+$ T cell recall. Based on studies revealing utility of $CD8^+$ T cell recall in mediating antiviral inflammation[1,2] and antitumor immunotherapy[3], we hypothesize that recall of Th1 polarizing vaccines will also parlay help to antitumor $CD8^+$ T cells, with the caveat that antitumor functions of type II immunity may be lacking. While Th1/Tc1, Th2/Tc2, and Th17/Tc17 polarizations are canonically known to mutually exclude one another, in the context of recall antigen therapy Th1 ($CD8^+$ T cell engagement, expression of Tbet/IFNγ by $CD4^+$ T cells); Th2 (recruitment of eosinophils and ILC2s, expression of GATA3 by $CD4^+$ T cells); and to a lesser extent, Th17 (RORγT expression in $CD4^+$ and $CD8^+$ T cells) polarizing features were observed. These findings support mounting evidence that diverse $CD4^+$ T cell polarizations generate compatible and productive immune responses[51-54].

Our study indicates that while pre-existing immunity dampens viral replication within the tumor, it contributes to overall superior antitumor efficacy of polio virotherapy. In line with our findings, recent reports demonstrated that the antitumor efficacy of Newcastle's Disease Virus (NDV) was enhanced in mice previously infected with NDV[4], despite reducing intratumor NDV replication, and inclusion of tetanus toxoid antigen in an oncolytic adenovirus potentiated antitumor efficacy in tet immunized mice[55]. Our work demonstrates that the antitumor effect of vaccine-specific recall

responses is contingent upon $CD4^+$ T cells; does not require direct infection of, or antigen presentation by, malignant cells; and mediates antitumor efficacy through both type I and II immunity. Our findings imply pre-existing immunity to PVSRIPO, due to routine pediatric immunization, is an asset to intratumor therapy that contributes a lysis-independent mechanism of action in cancer patients. Further investigations, particularly in clinical trials, are needed to determine the contribution of immunological recall responses to clinical benefit in a cancer immunotherapy setting.

Given the widely recognized importance of $CD4^+$ T cells in cancer immunotherapy[29,34], there are growing efforts to leverage $CD4^+$ T cell help within tumors. One approach in clinical development is that of CD40 agonistic antibodies[39]; notably, this approach targets one of many nodes engaged by $CD4^+$ T cell help, and polio recall-mediated antitumor efficacy independent of CD40L-CD40 signaling. Indeed, $CD4^+$ T cell help can promote dendritic cell and $CD8^+$ T cell activation/function in the absence of CD40[56]. The antitumor efficacy of cancer vaccines has been shown to be potentiated by including MHC class II epitopes[11], inspiring next generation vaccine designs that prime neoantigen specific $CD4^+$ and $CD8^+$ T cells[57]. Our work uncovers previously unrecognized potential of repurposing childhood vaccine-specific memory $CD4^+$ T cells to enlist $CD4^+$ T cell help for cancer immunotherapy.

Materials and Methods

Mice, cell lines, viruses, poly(I:C), and antibodies. hCD155-tg C57BL/6 mice were a gift of Satoshi Koike (Tokyo Metropolitan Institute of Medical Science, Japan). C57BL/6J mice (strain code: 000664), CD8 knockout C57BL/6 mice (strain code: 002665), B cell knockout C57BL/6 mice (strain code: 002288), OT-I C57BL/6 mice (strain code 03831), and CD45.1 C57BL/6 mice (strain code 002014) were purchased from The Jackson Laboratory. OT-I mice were crossed with CD45.1 C57BL/6 mice to generate CD45.1+ OT-I mice for use in these studies. All mice were used in accordance with Duke IACUC-approved protocols. B16.F10 (ATCC), E0771 (a gift from Greg Palmer, Duke University, USA), B16.F10^{hCD155}, and B16.F10.9^{hCD155}-OVA cells were grown in high-glucose DMEM (Gibco) supplemented with 10% FBS. B16.F10.9^{hCD155}-OVA and B16-F10^{hCD155} cells were derived by lentiviral transduction with CD155 as previously described[17]; B16-F10^{hCD155} cells were purified after transduction by FACs after staining with a hCD155-PE conjugated antibody (Biolegend). All cell lines were confirmed to be mycoplasma negative (Duke Cell Culture Facility). Laboratory, research grade, PVSRIPO and mRIPO viral stocks were generated and titered as previously described[58,59]. UV-inactivated PVSRIPO (UVP) was generated from PVSRIPO stock exposed to 39W UV-C germicidal lamp bulb (Sankyo Denki) in a biocontainment laminar flow hood at a distance of 4 ft for 4h; inactivation was confirmed via plaque assay comparison to input virus, and input virus titer was used to define the dose of UVP. The antigenicity of UVP was confirmed by measuring reactivity of human sera to UVP via immunoblot, comparing to input virus. VacciGrade^{TM} high molecular weight poly(I:C) (Invivogen) was reconstituted and annealed as recommended by the manufacturer; 30μg of poly(I:C) was delivered intratumor after mixing with either PBS or denoted antigen in the figure/figure legend. In vivo grade antibodies to IL-5 (Clone TRK5) or isotype control (Clone

HRPN), PD1 (Clone RMP1.14) or isotype control (Clone 2A3), CD40L (Clone MR-1) or isotype control (catalog# BP0091), and CD40 (Clone FGK4.5) or isotype control (Clone 2A3) were purchased from BioXcell and were delivered I.P. at the concentrations and frequencies described in figure legends.

Vaccines, immunizations, polio neutralizing antibody assay, ELISA, and intratumor viral titers. Unless otherwise indicated, polio immunization was achieved using PVSRIPO; Tetanus immunization was achieved using tetanus toxoid (Millipore-Sigma, reconstituted in sterile water); and KLH immunization was achieved using Hemocyanin-Keyhole Limpet (Sigma-Aldrich, reconstituted in PBS). PVSRIPO ($1x10^7$ plaque forming units/mouse), Tetanus toxoid (0.5 mg/mouse), or Hemocyanin-Keyhole Limpet (KLH, 100mg/mouse, Sigma-Aldrich) were prepared for immunization via dilution in PBS and mixed 1:1 with Alhydrogel (Invivogen) with vigorous pipetting for 2 min. For polio immunization excluding Alhydrogel in Fig 1B, the same procedure was performed with PBS. Clinical-grade Salk vaccine (IPOL^{TM}) and Tenivac® (Sanofi-Pasteur) were used at a dose of 100µl per mouse; for experiments using Salk + Aldhydrogel, Salk vaccine was mixed 1:1 with Alhydrogel followed by mixing and an effective dose of 50µl was administered/mouse. For all single antigen immunizations, 50µl of vaccine was administered bilaterally in the quadricep muscles (100µl total per immunization); combined immunization of Salk (IPOL^{TM}) and Tenivac was achieved via delivery to only one quadricep for each vaccine, using opposing quadriceps. After the initial immunization in 4-5 week old mice, repeat immunization/boost occurred 14 days later using the same dosing/preparation techniques. Thirty days after boost vaccination, tumors were implanted, or spleens were isolated (for adoptive transfer experiments) as described in experiment associated timelines in Figures/Figure legends. The polio neutralization assay was performed as previously described[60]. ELISA to measure anti-polio

antibodies was performed by coating ELISA plates (Maxisorp, Nunc) with $1x10^7$ pfu PVSRIPO per well overnight (4°C) in 0.5M carbonate bicarbonate buffer (pH 9.6); blocking in PBS containing 2% BSA + 0.05% Tween-20 (Sigma-Aldrich); dilution of sera at 1:20, 1:100, 1:500 and incubation for 2 hours at RT; washing in PBS + 0.05% Tween 20; followed by incubation with 1:30,000 protein-A conjugated HRP (Thermo-Fisher) diluted in PBS for 1h; washing, and development using TMB substrate (Thermo-Fisher). A similar procedure was used for detection of KLH antibodies and Tetanus-specific antibodies, coating plates at a concentration of 10 or 1μg/ml antigen, respectively. To determine intratumor viral titers, tumors were harvested at the denoted time points, weighed, and mechanically homogenized in 1ml PBS. Supernatant resulting from homogenization and two freeze-thaw cycles (-80°C, to ensure cell lysis) was tested by plaque assay as previously described[58] using a starting dilution of 1:100; higher dilutions resulted in confounding HeLa cell death likely due to tumor debris. Viral neutralization titers/ml were divided by tumor weight (g) for presentation in figures.

Murine tumor model experiments. For B16 tumor implantation $2x10^5$ cells in 50μl PBS were implanted subcutaneously into the right flank; for E0771 tumor implantations $5x10^5$ cells in 50μl PBS were implanted into the 4th mammary fat pad. Male hCD155-tg C57BL/6 mice were used for B16 studies, female mice were used for studies in wt C57BL/6 mice and for all E0771 studies to enable orthotopic fat pad implantation, and female mice were used for adoptive transfer experiments (donors and recipients). Tumors were treated according to timelines presented in figures; generally, tumors were treated upon reaching a volume of ~20-40mm^3 with either mRIPO ($1x10^7$ pfu), UVP ($1x10^8$ inactivated pfu), Tetanus toxoid (0.5 μg), and/or poly(I:C) (30 μg) as indicated in figures/figure legends. DMEM (dilution media for mRIPO and UVP) was injected in a similar manner for mock controls. Treatment groups were randomized by tumor volume at the

first day of treatment. In some experiments, groups of mice were treated at different time points after tumor implant due to heterogenous tumor growth, possibly because of the older age of mice used in this study. In these circumstances, each treatment group had equal numbers on each treatment day and the earliest treatment date is depicted in the figure/figure legend. Tumor volume was measured using vernier calipers and calculated using the equation (L x W x W)/2; mice were euthanized upon reaching tumor volume of 1000mm^3. Tumor measurements were performed blinded to treatment group designations beginning after the last dose of intratumor therapy/antigen.

Flow cytometry analysis of tumors and TDLNs. Tumors were harvested at time points denoted in figures/figure legends and dissociated in RPMI-1640 media (Thermo-Fisher) containing 100µg/ml Liberase-TM (Sigma-Aldrich) and 10µg/ml DNAse I (Roche) for 30min at 37°C with agitation, followed by filtering through a 70µM (Olympus Plastics) cell strainer, centrifugation, and washing in PBS. TDLNs were crushed in 1ml RPMI + 10% FBS in a 70µm cell strainer followed by washing in PBS. For experiments using Zombie-Aqua, cells were stained with Zombie-Aqua in PBS followed by washing in FACs buffer (PBS + 2% FBS) for downstream processing. Single cell suspensions were then incubated with 1:50 mouse Tru-stain FcX^{TM} (Biolegend) in FACs buffer, followed by division of cell suspension for staining in multiple panels. The panels used in this study include antibodies to the following antigens (purchased from Biolegend unless otherwise noted): lineage panel 1: CD45.2-BUV395 and CD40-BV605 (BD biosciences), Zombie-Aqua Live/dead, NK1.1-BV421, CD11b-BV711, IA/IE-BV786, CD19-FITC, LY6G-PE, F4/80-PE, CD86-PEcy7, CD3-APC; lineage panel 2: CD19-BUV395 (BD biosciences), 7-AAD, CD45.2-APC-Cy7, CD11b-BV711, LY6C-PerCP-Cy5.5, LY6G-PE, CD3-FITC, CD11c-APC; lineage panel 3: CD45.2-BUV395 and CD40-BV605 (BD biosciences), Zombie-Aqua Live/dead, NK1.1-

BV421, CD11b-BV711, IA/IE-BV786, CD3/CD19-FITC, LY6G-PE, F4/80-PE, CD86-PEcy7, CD11c-APC; T cell panel: CD45.2-BUV395, Zombie-Aqua Live/dead, CD3-PE, CD4-FITC, CD8-BV421, CD69-BV605, PD1-PE-Cy7 (Thermo-Fisher), TIM3-BV711, CD44-PE-Cy5; Intracellular staining T cell panel 1: CD45.2-BUV395, Zombie-Aqua Live/dead, CD3-APC, CD4-FITC, CD8-BV421, FoxP3-PE-Cy5 (Thermo-Fisher), IFN-γ-BV786, TNF-BV605, Granzyme B-PE-Cy7; intracellular staining T cell panel 2: CD45.2-BUV395, Zombie-Aqua Live/dead, CD3-APC, CD4-FITC, CD8-BV42, FoxP3-PE-Cy5, Tbet-BV711, GATA3-PE, IRF4-PerCP-Cy5.5, RoRγT-BV786, and BCL6-PE-Cy7; OT-I T cell panels were accomplished using the three above T cell panels with exchange of CD45.2 for CD45.1-BUV395; Eosinophils panel: CD45.2-BUV395, CCR3-BV421, Zombie Aqua, CD3/CD19/NK1.1-BV510, CD11c-BV605, CD11b-BV711, IA/IE-BV786, Siglec F-AF488, Ly6C-PERCP-Cy5.5, CD103-PE, F4/80-PECy5, PD1-PEcy7, PD-L1-APC; and ILC2 panel: CD45.2-BUV395, Zombie Aqua, CD3/CD5/CD19/NK1.1/ CD11c/CD11b/FCεRIa/γδTCR/αβTCR-BV510, ST-2(IL33R)-BV605, CD25-BV711, PD1-BV786, CD90.2-AF488, IL5-PE, CD127-PEcy5, Granzyme B-PECy7, KLRG1-APC. Flow cytometry experiments were performed using a Fortessa X20 at the Duke Cancer Institute Flow Cytometry Core Facility; FCS files were analyzed using Flow-Jo version 10 (BD Biosciences). VersaComp beads (Beckmann-Coulter) and staining of fresh blood were used to establish panel compensation, which was then optimized using florescence minus one isotype controls. Gating strategies are presented in supplemental materials; isotype controls, fluorescence minus one controls, and comparison to established negative cell populations were used to define positivity for markers of interest.

PBMC studies. For healthy donor analyses, leukopaks (Stemcell Technologies) from 5 different de-identified donors were processed using Leucosep™ tubes (Greiner Bio-One) and Ficoll-

Paque™ Plus (GE healthcare) to isolate PBMCs following the manufacturer's instructions. Luekopaks were collected under an approved IRB protocol held by Stemcell Technologies, Inc, and were provided for these studies in a deidentified manner. PBMCs were thawed, washed in Aim-V media (Thermo-Fisher), and incubated in 1 ml AIM-V media containing 10μg/ml DNAse I (Roche). Cells were then washed in RPMI-1640 containing 10% FBS and plated at a density of $1x10^7$ PBMCs in 2ml RPMI-1640 + 10% FBS per well in a 6-well plate, followed by addition of nothing (mock), recall antigens (1μg/ml Tetanus toxoid; $1x10^8$ inactivated titer, or 50ul of IPOL™ vaccine), or Poly I:C (10μg/ml). Six days later, supernatant was retained for cytokine measurement. For PBMC studies from recurrent GBM patients, PBMCs collected under an IRB approved protocol (Duke University) and were thawed and processed as done for healthy donors, but plated at a density of $1x10^5$ cells per well in a 96 well plate and treated with mock, UVP, or Tetanus at the concentrations noted above for 3 days; a companion set of age and sex matched deidentfied PBMCs from 10 healthy donors (Stemcell Tech; IRB approved protocol held by the vendor) were included for comparison along with batch control leukophoresis derived PBMCs. Cytokines were measured using the Human Antiviral, Human Pro-Inflammatory Chemokine, and Human Th LegendPlex™ kits (Biolegend) following the manufacturer's instructions, and analyzed using LegendPlex software (Biolegend).

Adoptive transfer studies and RNA sequencing of tumor infiltrating OT-I T cells. For adoptive transfer of $CD4^+$ T cells from polio or Tet immunized mice (Fig 4E, Fig S6), following prime (Day -45) and boost (Day -31) with either tetanus/KLH vs PVSRIPO + Alhydrogel immunization as described above, mice were euthanized, and spleens (two each) were harvested. Separately, hCD155-tg C57BL/6 mice were implanted with B16.F10.9^{hCD155} tumors six days prior to splenocyte isolation. Spleens from immunized mice were crushed through a 70μm cell strainer in

3ml RPMI-1640. Resulting cell pellets were reconstituted in 2ml ACK red blood cell lysis buffer (Lonza) and incubated for 10 min at RT, followed by addition of 10ml RPMI and centrifugation. $CD4^+$ T cells were negatively selected from single cell suspensions using the EasySep^{TM} $CD4^+$ T cell isolation kit (Stemcell Technologies) following the manufacturer's instructions. Two million $CD4^+$ T cells were injected intraperitoneally six days after $B16^{hCD155}$ tumor implantation. Seven days after tumor implantation, recipient mice were treated with mock (DMEM) or mRIPO ($1x10^7$ pfu) and tumor growth was monitored. For adoptive transfer of OT-I x CD45.1 cells, spleens from OT-I x CD45.1 mice were harvested and processed to single cell suspensions as described above. OT-I splenocytes were treated with 10µg/ml SIINFEKL peptide (Invivogen) for 16h, washed in PBS, and then $2x10^6$ OT-I splenocytes were transferred in 100µl i.p. For transfer of T cells from mice treated with recall antigen therapy (Fig 5E), splenocytes were processed as described above, washed in PBS, and transferred to naïve recipients immediately following subcutaneous injection of B16.F10.9-OVA cells. For analysis of OT-I T cell transcriptomes after polio recall, mice immunized against polio (PVSRIPO, $1x10^7$ pfu in alhydrogel) 45 days (prime) and 30 days (boost) prior to B16-OVA tumor implantation received SIINFEKL-activated OT-I splenocytes as described above, and were treated with intratumor mock (PBS) or UVP 9 days after tumor implantation. Twelve days post-treatment tumors were dissociated and subjected to CD45.1 positive selection (MojoSort mouse CD45.1 selection kit, Biolegend) per the manufacterer's instructions. A subset of the isolated cells were analyzed by flow cytometry using the following panel: 7-AAD, CD45.2-BUV395 (BD Biosciences), CD3-PE, CD8-BV421, CD4-FITC (Biolegend unless otherwise specified); the remaining cells were lysed in 200µl Trizol (Thermo-Fisher). Cholorform extracted RNA from trizol samples (per manufacterer's instructions) was purified using the RNEasy kit (Qiagen, Inc.) and analyzed on a Hi-seq Illumini sequencer (150bp,

PE) at Azenta Life Sciences. Transcripts were aligned with STAR (v2.7) to the GRCm38 mouse genome and differential expression analysis was performed using DESeq2 (v 1.34). These isolations and downstream analyses were performed for two independent expeirments: in one experiment mock treatment was compared to UVP, in a separate experiment Tet treatment was compared to UVP treatment, both in polio immunized mice.

Associations of eosinophils with other cell types in human tumors and survival. CIBERSORT predicted cell type enrichment for each cancer type were obtained from Thorsson et al[35]. Within each cancer type, cases were sorted by eosinophil enrichment, and comparisons were performed between cases with eosinophil score = 0 (EO^{Neg}) vs eosinophil score >0 (EO+). Total CD4+ T cells reflects the sum of the following scores: 'T cells CD4 Memory Activated' + 'T cells CD4 Memory Resting' + 'T cells CD4 Naïve' + 'T cells follicular helper.' For pan-cancer analyses mean enrichment values for each cell type were determined for EO^{Neg} and EO+ for comparison and plotting in Fig 6A. Mean values from each cell type were scaled and centered within each cell type score across all samples (both EO^{Neg} and EO+), followed by subtracting normalized EO+ from EO^{Neg} values to to generate heatmaps in Fig S9B and Fig S10A. False discovery rate (Benjamini-Hochberg method) was used to adjust for multiple comparisons in Figs S9B and S10A.

Statistical analysis. Assay-specific statistical tests are indicated in the corresponding figure legends. GraphPad Prism 8 was used to perform all statistical analyses and plot data. A statistical probability of <0.05 ($p<0.05$) was used unless otherwise noted. All data points reflect individual specimens, experimental repeats, or mice.

Acknowledgements: We thank G. Palmer (Duke University, NC) for providing the E0771 cell line, M. Mohme (University of Hamburg Medical Center, Hamburg, Germany) for technical

advice, and Satoshi Koike (Tokyo Metropolitan Institute of Medical Science, Japan) for hCD155-tg C57BL6 mice. **Funding:** PHS: F32CA224593 (M.C.B.), K99CA263021 (M.C.B.), R01NS108773 (M.G. and S.K.N.), R35CA225622 (D.D.B.); Department of Defense Breast Cancer Research Program award W81XWH-16-1-0354 (S.K.N.), National Cancer Center Breast Cancer Project Grant (M.C.B.).

References

1 Schenkel, J. M. *et al.* T cell memory. Resident memory CD8 T cells trigger protective innate and adaptive immune responses. *Science* **346**, 98-101, doi:10.1126/science.1254536 (2014).

2 Ariotti, S. *et al.* T cell memory. Skin-resident memory CD8(+) T cells trigger a state of tissue-wide pathogen alert. *Science* **346**, 101-105, doi:10.1126/science.1254803 (2014).

3 Rosato, P. C. *et al.* Virus-specific memory T cells populate tumors and can be repurposed for tumor immunotherapy. *Nat Commun* **10**, 567, doi:10.1038/s41467-019-08534-1 (2019).

4 Ricca, J. M. *et al.* Pre-existing Immunity to Oncolytic Virus Potentiates Its Immunotherapeutic Efficacy. *Mol Ther* **26**, 1008-1019, doi:10.1016/j.ymthe.2018.01.019 (2018).

5 Mitchell, D. A. *et al.* Tetanus toxoid and CCL3 improve dendritic cell vaccines in mice and glioblastoma patients. *Nature* **519**, 366-369, doi:10.1038/nature14320 (2015).

6 Lorvik, K. B. *et al.* Adoptive Transfer of Tumor-Specific Th2 Cells Eradicates Tumors by Triggering an In Situ Inflammatory Immune Response. *Cancer Res* **76**, 6864-6876, doi:10.1158/0008-5472.CAN-16-1219 (2016).

7 Mackensen, A. *et al.* Phase I study of adoptive T-cell therapy using antigen-specific CD8+ T cells for the treatment of patients with metastatic melanoma. *J Clin Oncol* **24**, 5060-5069, doi:10.1200/JCO.2006.07.1100 (2006).

8 Simon, S. C. S. *et al.* Eosinophil accumulation predicts response to melanoma treatment with immune checkpoint inhibitors. *Oncoimmunology* **9**, 1727116, doi:10.1080/2162402X.2020.1727116 (2020).

9 Moral, J. A. *et al.* ILC2s amplify PD-1 blockade by activating tissue-specific cancer immunity. *Nature* **579**, 130-135, doi:10.1038/s41586-020-2015-4 (2020).

10 Jacquelot, N. *et al.* Blockade of the co-inhibitory molecule PD-1 unleashes ILC2-dependent antitumor immunity in melanoma. *Nat Immunol* **22**, 851-864, doi:10.1038/s41590-021-00943-z (2021).

11 Alspach, E. *et al.* MHC-II neoantigens shape tumour immunity and response to immunotherapy. *Nature* **574**, 696-701, doi:10.1038/s41586-019-1671-8 (2019).

12 Gromeier, M., Lachmann, S., Rosenfeld, M. R., Gutin, P. H. & Wimmer, E. Intergeneric poliovirus recombinants for the treatment of malignant glioma. *Proc Natl Acad Sci U S A* **97**, 6803-6808, doi:10.1073/pnas.97.12.6803 (2000).

13 Desjardins, A. *et al.* Recurrent Glioblastoma Treated with Recombinant Poliovirus. *N Engl J Med* **379**, 150-161, doi:10.1056/NEJMoa1716435 (2018).

14 Beasley, G. M. *et al.* Phase I trial of intratumoral PVSRIPO in patients with unresectable, treatment-refractory melanoma. *J Immunother Cancer* **9**, doi:10.1136/jitc-2020-002203 (2021).

15 Brown, M. C. *et al.* Viral infection of cells within the tumor microenvironment mediates antitumor immunotherapy via selective TBK1-IRF3 signaling. *Nat Commun* **12**, 1858, doi:10.1038/s41467-021-22088-1 (2021).

16 Ochiai, H. *et al.* Treatment of intracerebral neoplasia and neoplastic meningitis with regional delivery of oncolytic recombinant poliovirus. *Clin Cancer Res* **10**, 4831-4838, doi:10.1158/1078-0432.CCR-03-0694 (2004).

17 Brown, M. C. *et al.* Cancer immunotherapy with recombinant poliovirus induces IFN-dominant activation of dendritic cells and tumor antigen-specific CTLs. *Sci Transl Med* **9**, doi:10.1126/scitranslmed.aan4220 (2017).

18 Holl, E. K. *et al.* Recombinant oncolytic poliovirus, PVSRIPO, has potent cytotoxic and innate inflammatory effects, mediating therapy in human breast and prostate cancer xenograft models. *Oncotarget* **7**, 79828-79841, doi:10.18632/oncotarget.12975 (2016).

19 Hawken, J. & Troy, S. B. Adjuvants and inactivated polio vaccine: a systematic review. *Vaccine* **30**, 6971-6979, doi:10.1016/j.vaccine.2012.09.059 (2012).

20 Swain, S. L. Generation and in vivo persistence of polarized Th1 and Th2 memory cells. *Immunity* **1**, 543-552, doi:10.1016/1074-7613(94)90044-2 (1994).

21 Mosaheb, M. M. *et al.* Genetically stable poliovirus vectors activate dendritic cells and prime antitumor CD8 T cell immunity. *Nat Commun* **11**, 524, doi:10.1038/s41467-019-13939-z (2020).

22 Mittrucker, H. W. *et al.* Requirement for the transcription factor LSIRF/IRF4 for mature B and T lymphocyte function. *Science* **275**, 540-543, doi:10.1126/science.275.5299.540 (1997).

23 Nimmerjahn, F. & Ravetch, J. V. Fcgamma receptors as regulators of immune responses. *Nat Rev Immunol* **8**, 34-47, doi:10.1038/nri2206 (2008).

24 Cachot, A. *et al.* Tumor-specific cytolytic CD4 T cells mediate immunity against human cancer. *Sci Adv* **7**, doi:10.1126/sciadv.abe3348 (2021).

25 Oh, D. Y. *et al.* Intratumoral CD4(+) T Cells Mediate Anti-tumor Cytotoxicity in Human Bladder Cancer. *Cell* **181**, 1612-1625 e1613, doi:10.1016/j.cell.2020.05.017 (2020).

26 Quezada, S. A. *et al.* Tumor-reactive CD4(+) T cells develop cytotoxic activity and eradicate large established melanoma after transfer into lymphopenic hosts. *J Exp Med* **207**, 637-650, doi:10.1084/jem.20091918 (2010).

27 Perez-Diez, A. *et al.* CD4 cells can be more efficient at tumor rejection than CD8 cells. *Blood* **109**, 5346-5354, doi:10.1182/blood-2006-10-051318 (2007).

28 Corthay, A. *et al.* Primary antitumor immune response mediated by CD4+ T cells. *Immunity* **22**, 371-383, doi:10.1016/j.immuni.2005.02.003 (2005).

29 Borst, J., Ahrends, T., Babala, N., Melief, C. J. M. & Kastenmuller, W. CD4(+) T cell help in cancer immunology and immunotherapy. *Nat Rev Immunol* **18**, 635-647, doi:10.1038/s41577-018-0044-0 (2018).

30 Ahrends, T. *et al.* CD4(+) T Cell Help Confers a Cytotoxic T Cell Effector Program Including Coinhibitory Receptor Downregulation and Increased Tissue Invasiveness. *Immunity* **47**, 848-861 e845, doi:10.1016/j.immuni.2017.10.009 (2017).

31 Ahrends, T. *et al.* CD4(+) T cell help creates memory CD8(+) T cells with innate and help-independent recall capacities. *Nat Commun* **10**, 5531, doi:10.1038/s41467-019-13438-1 (2019).

32 Church, S. E., Jensen, S. M., Antony, P. A., Restifo, N. P. & Fox, B. A. Tumor-specific CD4+ T cells maintain effector and memory tumor-specific CD8+ T cells. *Eur J Immunol* **44**, 69-79, doi:10.1002/eji.201343718 (2014).

33 Arnold, I. C. *et al.* The GM-CSF-IRF5 signaling axis in eosinophils promotes antitumor immunity through activation of type 1 T cell responses. *J Exp Med* **217**, doi:10.1084/jem.20190706 (2020).

34 Hung, K. *et al.* The central role of CD4(+) T cells in the antitumor immune response. *J Exp Med* **188**, 2357-2368, doi:10.1084/jem.188.12.2357 (1998).

35 Thorsson, V. *et al.* The Immune Landscape of Cancer. *Immunity* **48**, 812-830 e814, doi:10.1016/j.immuni.2018.03.023 (2018).

36 Newman, A. M. *et al.* Determining cell type abundance and expression from bulk tissues with digital cytometry. *Nat Biotechnol* **37**, 773-782, doi:10.1038/s41587-019-0114-2 (2019).

37 Oliphant, C. J. *et al.* MHCII-mediated dialog between group 2 innate lymphoid cells and CD4(+) T cells potentiates type 2 immunity and promotes parasitic helminth expulsion. *Immunity* **41**, 283-295, doi:10.1016/j.immuni.2014.06.016 (2014).

38 Moynihan, K. D. *et al.* Eradication of large established tumors in mice by combination immunotherapy that engages innate and adaptive immune responses. *Nat Med* **22**, 1402-1410, doi:10.1038/nm.4200 (2016).

39 Vonderheide, R. H. CD40 Agonist Antibodies in Cancer Immunotherapy. *Annu Rev Med* **71**, 47-58, doi:10.1146/annurev-med-062518-045435 (2020).

40 Laidlaw, B. J., Craft, J. E. & Kaech, S. M. The multifaceted role of CD4(+) T cells in CD8(+) T cell memory. *Nat Rev Immunol* **16**, 102-111, doi:10.1038/nri.2015.10 (2016).

41 Lloyd, C. M. & Hessel, E. M. Functions of T cells in asthma: more than just T(H)2 cells. *Nat Rev Immunol* **10**, 838-848, doi:10.1038/nri2870 (2010).

42 Smith, S. G. *et al.* Increased numbers of activated group 2 innate lymphoid cells in the airways of patients with severe asthma and persistent airway eosinophilia. *J Allergy Clin Immunol* **137**, 75-86 e78, doi:10.1016/j.jaci.2015.05.037 (2016).

43 Carretero, R. *et al.* Eosinophils orchestrate cancer rejection by normalizing tumor vessels and enhancing infiltration of CD8(+) T cells. *Nat Immunol* **16**, 609-617, doi:10.1038/ni.3159 (2015).

44 Hartl, D. *et al.* Quantitative and functional impairment of pulmonary CD4+CD25hi regulatory T cells in pediatric asthma. *J Allergy Clin Immunol* **119**, 1258-1266, doi:10.1016/j.jaci.2007.02.023 (2007).

45 Entwistle, L. J. *et al.* Pulmonary Group 2 Innate Lymphoid Cell Phenotype Is Context Specific: Determining the Effect of Strain, Location, and Stimuli. *Front Immunol* **10**, 3114, doi:10.3389/fimmu.2019.03114 (2019).

46 de Lucia Finkel, P., Xia, W. & Jefferies, W. A. Beyond Unconventional: What Do We Really Know about Group 2 Innate Lymphoid Cells? *J Immunol* **206**, 1409-1417, doi:10.4049/jimmunol.2000812 (2021).

47 Lim, A. I. *et al.* IL-12 drives functional plasticity of human group 2 innate lymphoid cells. *J Exp Med* **213**, 569-583, doi:10.1084/jem.20151750 (2016).

48 Ercolano, G. *et al.* PPAR drives IL-33-dependent ILC2 pro-tumoral functions. *Nat Commun* **12**, 2538, doi:10.1038/s41467-021-22764-2 (2021).

49 Trabanelli, S., Chevalier, M. F., Derre, L. & Jandus, C. The pro- and anti-tumor role of ILC2s. *Semin Immunol* **41**, 101276, doi:10.1016/j.smim.2019.04.004 (2019).

50 Simon, S. C. S., Utikal, J. & Umansky, V. Opposing roles of eosinophils in cancer. *Cancer Immunol Immunother* **68**, 823-833, doi:10.1007/s00262-018-2255-4 (2019).

51 Peine, M. *et al.* Stable T-bet(+)GATA-3(+) Th1/Th2 hybrid cells arise in vivo, can develop directly from naive precursors, and limit immunopathologic inflammation. *PLoS Biol* **11**, e1001633, doi:10.1371/journal.pbio.1001633 (2013).

52 Tuzlak, S. *et al.* Repositioning TH cell polarization from single cytokines to complex help. *Nat Immunol* **22**, 1210-1217, doi:10.1038/s41590-021-01009-w (2021).

53 Messi, M. *et al.* Memory and flexibility of cytokine gene expression as separable properties of human T(H)1 and T(H)2 lymphocytes. *Nat Immunol* **4**, 78-86, doi:10.1038/ni872 (2003).

54 Baumgarth, N., Brown, L., Jackson, D. & Kelso, A. Novel features of the respiratory tract T-cell response to influenza virus infection: lung T cells increase expression of gamma interferon mRNA in vivo and maintain high levels of mRNA expression for interleukin-5 (IL-5) and IL-10. *J Virol* **68**, 7575-7581 (1994).

55 Tahtinen, S. *et al.* Exploiting Preexisting Immunity to Enhance Oncolytic Cancer Immunotherapy. *Cancer Res* **80**, 2575-2585, doi:10.1158/0008-5472.CAN-19-2062 (2020).

56 Lu, Z. *et al.* CD40-independent pathways of T cell help for priming of CD8(+) cytotoxic T lymphocytes. *J Exp Med* **191**, 541-550, doi:10.1084/jem.191.3.541 (2000).

57 Ott, P. A. *et al.* An immunogenic personal neoantigen vaccine for patients with melanoma. *Nature* **547**, 217-221, doi:10.1038/nature22991 (2017).

58 Brown, M. C. *et al.* Induction of viral, 7-methyl-guanosine cap-independent translation and oncolysis by mitogen-activated protein kinase-interacting kinase-mediated effects on the serine/arginine-rich protein kinase. *J Virol* **88**, 13135-13148, doi:10.1128/jvi.01883-14 (2014).

59 Brown, M. C., Dobrikov, M. I. & Gromeier, M. Mitogen-activated protein kinase-interacting kinase regulates mTOR/AKT signaling and controls the serine/arginine-rich protein kinase-responsive type 1 internal ribosome entry site-mediated translation and viral oncolysis. *J Virol* **88**, 13149-13160, doi:10.1128/JVI.01884-14 (2014).

60 Boone, E. J. & Albrecht, P. Conventional and enhanced plaque neutralization assay for polio antibody. *J Virol Methods* **6**, 193-202, doi:10.1016/0166-0934(83)90046-0 (1983).

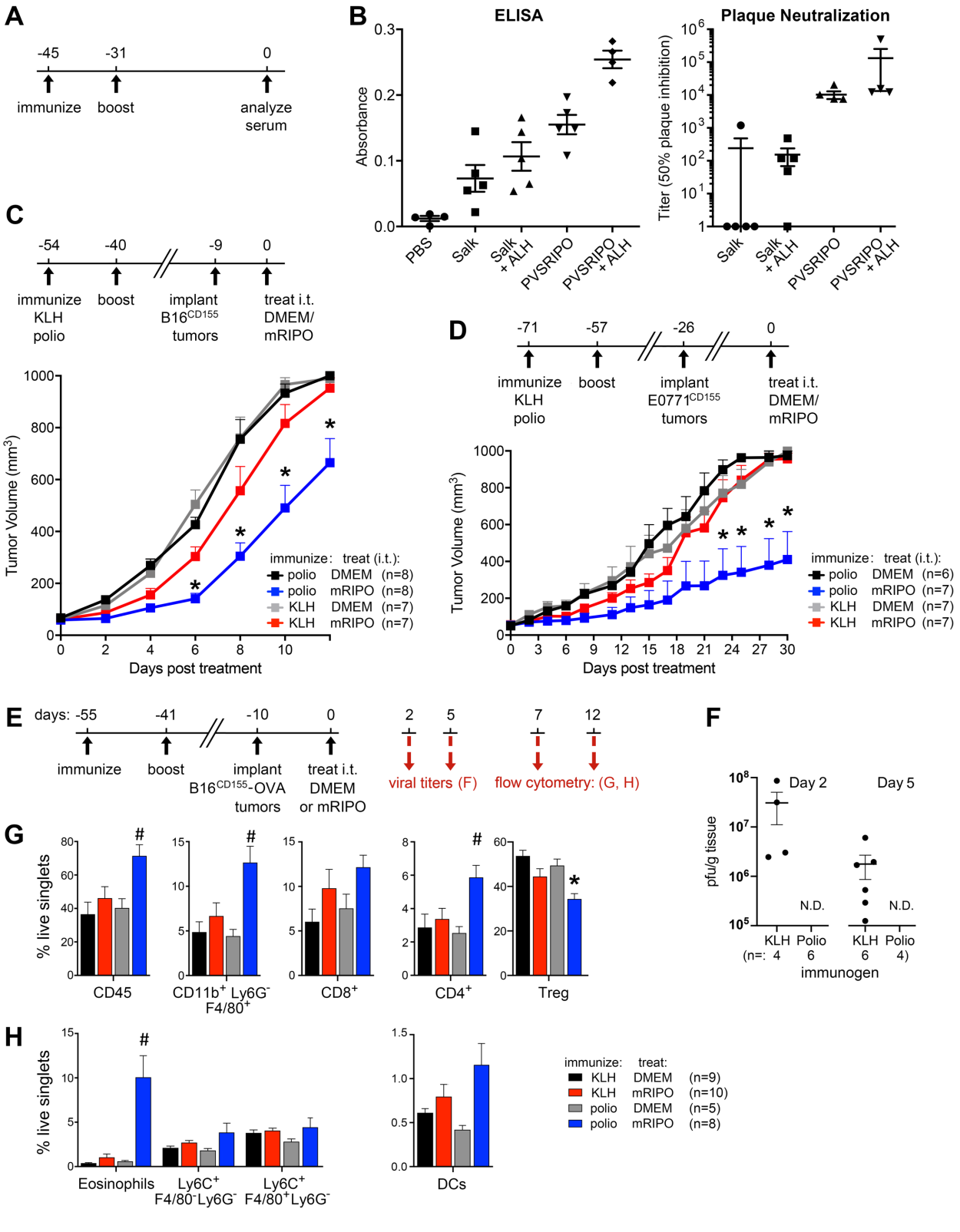

Figure 1. Polio immunization potentiates anti-tumor and inflammatory efficacy of recombinant poliovirus therapy. (**A**) Schema for immunization validation in (B). (**B**) ELISA (left) and plaque neutralization assay (right) from serum of mice immunized as shown (n= 5/group). (**C, D**) Polio (PVSRIPO + ALH) or KLH (KLH + ALH) immunized hCD155-tg C57BL/6 mice bearing hCD155-tg B16 (**C**, subcutaneous) or E0771 (**D**, fat pad) tumors were treated with DMEM (negative control) or mRIPO ($1x10^7$ pfu). Tumor growth was monitored; mean tumor volume + SEM are shown. Representative experiments from at least two repeats are depicted. (**E**) Schema for mechanistic analyses presented in F-H. (**F**) Tumor homogenates at 2- and 5-days post-mRIPO injection were tested for the presence of infectious virus by plaque assay; N.D.= not detected by the assay. (**G, H**) Flow cytometry analyses of tumors 7 days after mRIPO treatment for immune cell density. The results were confirmed in 3 independent experiments, a representative series is shown. Figures S1-3 present extended data and gating strategy. (**C, D**) Asterisks denote Dunnett's multiple comparison test vs all other groups ($p<0.05$, two tailed); (**G, H**) symbols indicate significant Tukey's post-hoc test vs mock controls (*) or all other groups (#). Data bars and brackets indicate mean + SEM.

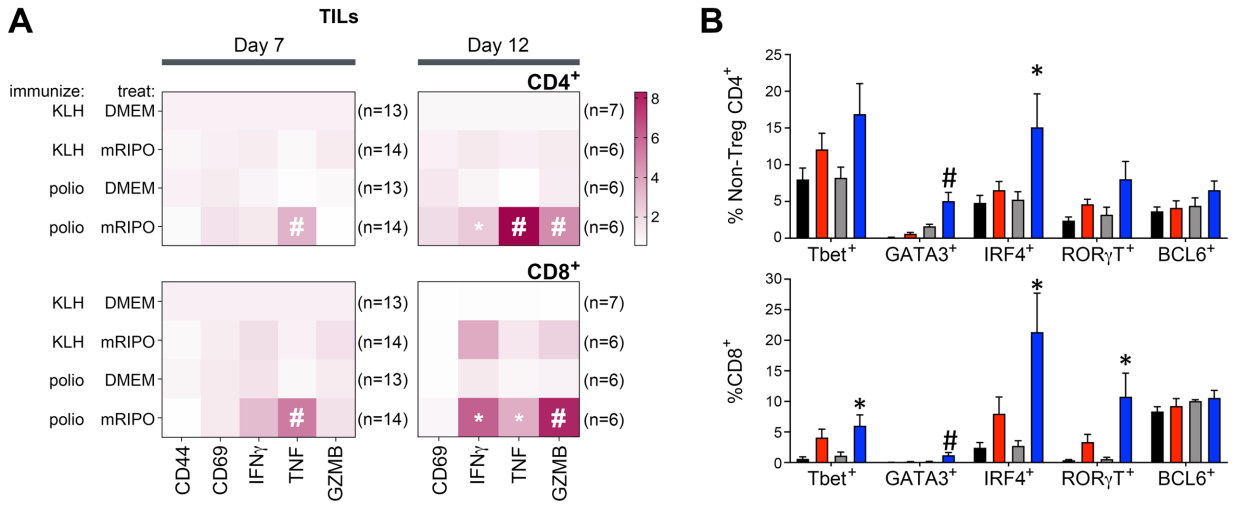

Figure 2. Accentuated T cell function and differentiation in polio-immunized mice treated with mRIPO. (**A-B**) TILs from the experiment shown in Figure 1E-H were analyzed for activation and differentiation markers. (**A**) Analysis of T cell activation markers in $CD4^+$ and $CD8^+$ TILs at days 7 and 12 post-treatment as indicated; samples were pooled from 2 experiments. Values were normalized as fold mean KLH-DMEM values for each marker. (**B**) Intracellular staining for relevant T cell-associated transcription factors was performed on $CD4^+$ (left) and $CD8^+$ (right) TILs 12 days after mRIPO therapy; same samples as in day 12 of (A). Data bars indicate mean + SEM. (**A**, **B**) Symbols indicate significant Tukey's post-hoc test relative to all other groups (#) or respective DMEM control (*). Figure S2D-E presents extended data; Fig S4 shows gating strategy.

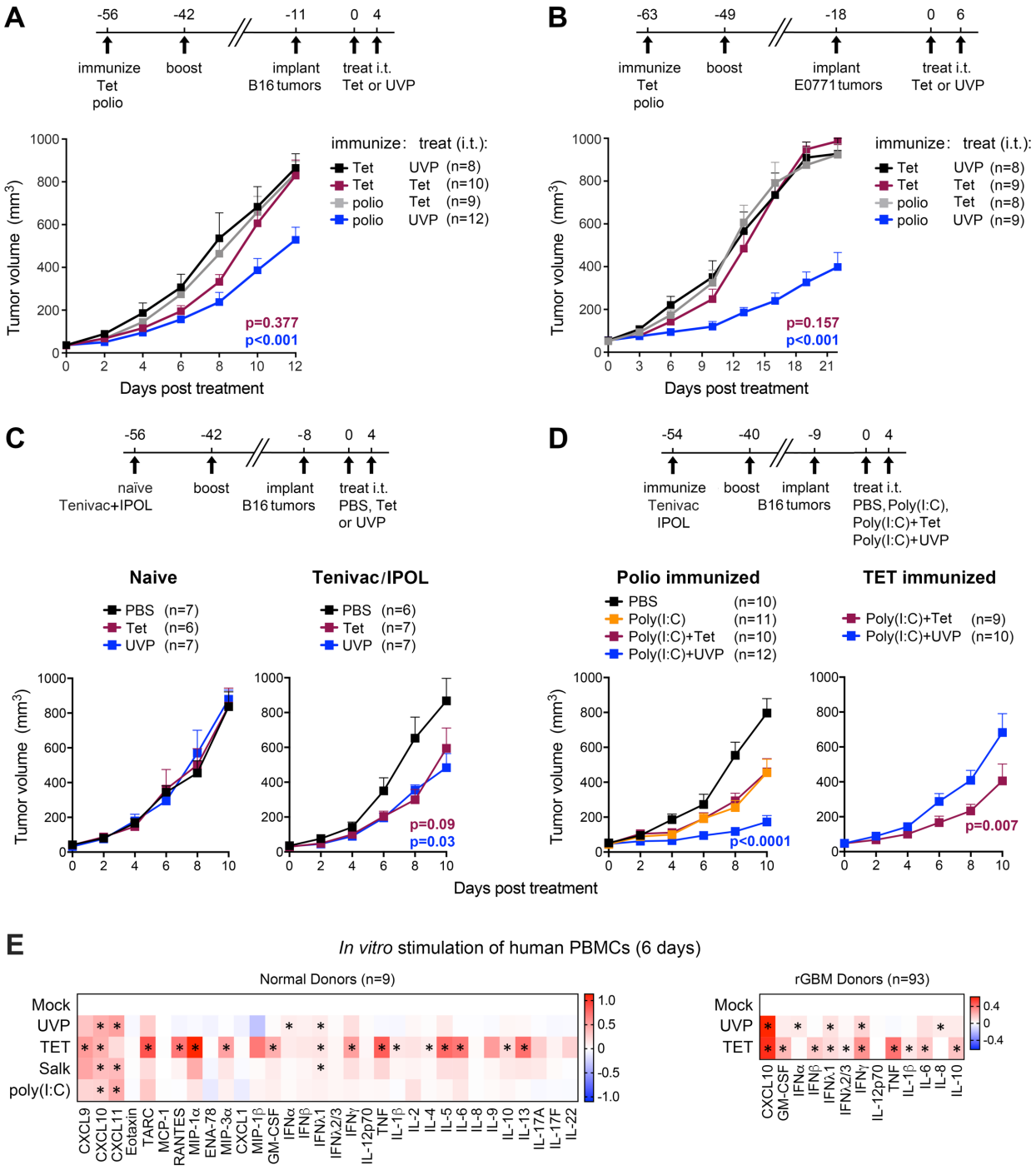

Figure 3. Polio and tetanus recall antigens mediate antitumor efficacy. B16 (**A**) or E0771 (**B**) tumor-bearing mice immunized with polio (PVSRIPO + ALH) or Tet (Tetanus toxoid + ALH) were treated intratumor with Tet (tetanus toxoid) or UVP (UV-inactivated PVSRIPO) as shown. (**C**) Age-matched naïve or Tenivac and IPOL^{TM} immunized mice were treated with PBS, Tet, or UVP as shown. (**D**) Mice

immunized as in (A, B) were treated intratumor with mock, poly(I:C) (30μg), poly(I:C) + Tet, or poly(I:C) + UVP as shown. (**E-F**) Human PBMCs from healthy donors (n= 9 tests from 5 different donors) or recurrent GBM patients were treated with mock, UVP ($1x10^8$ inactivated), or Tet (1μg/ml) for 6 or 3 days, respectively, *in vitro*. Supernatant cytokines were measured and are presented as log-fold mock control; asterisks denote significant Tukey's post hoc test. (**A-D**) Mean + SEM are shown and a representative experiment of at least two repeats is shown; asterisks indicate Dunnett's multiple comparison test $p<0.05$ (two tailed) vs all other groups. **Figure S5** presents related data.

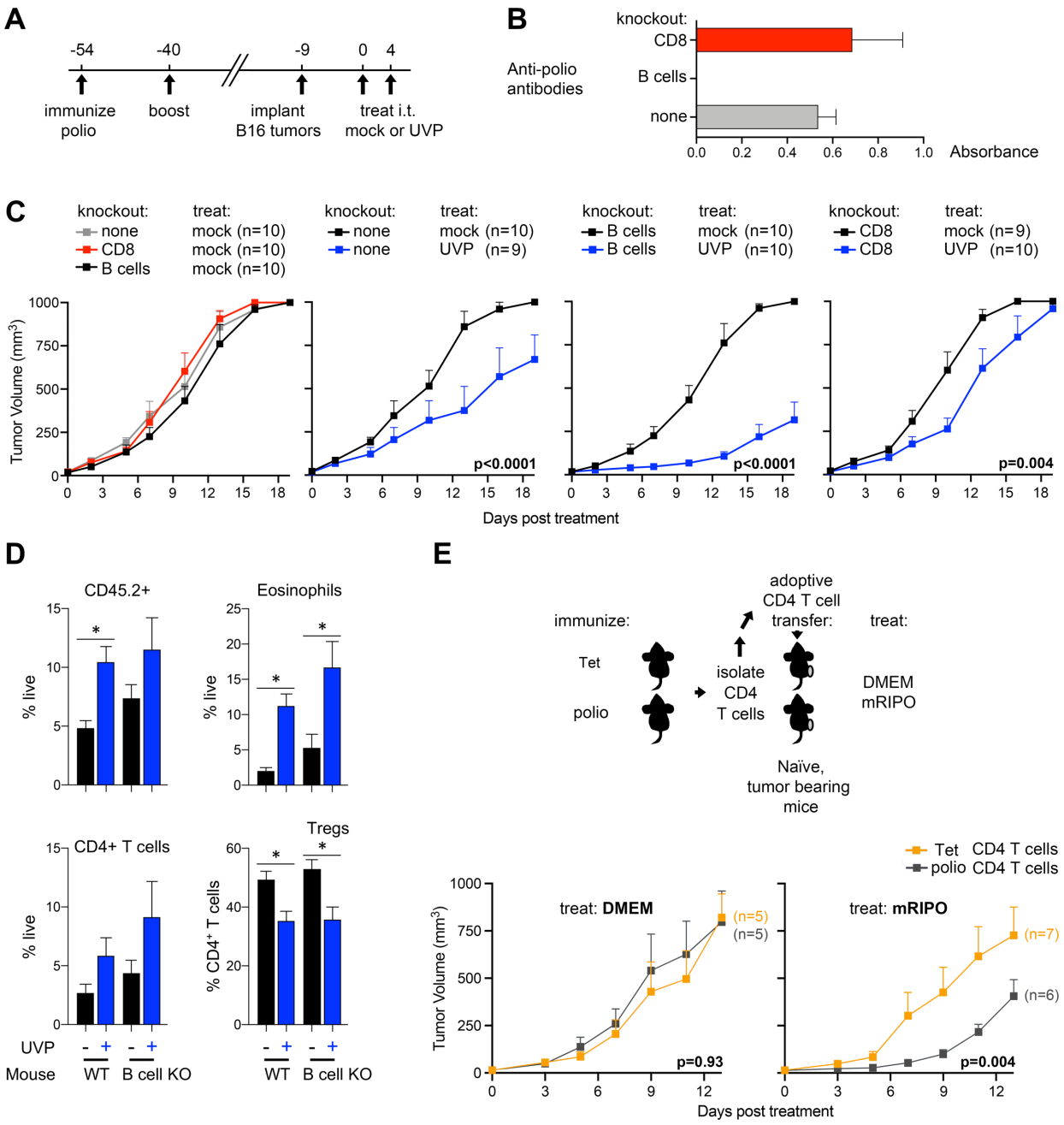

Figure 4. CD4$^+$ T cells mediate antitumor efficacy of polio recall. (**A**) Schema depicting experimental design for tumor growth experiments in wt, CD8$^+$ T cell k/o, or B cell k/o mice presented in (B, C). (**B**) ELISA for serum anti-polio antibodies in animals of each genetic background at the time of tumor implantation (n= 4/group). (**C**) Mean tumor volume + SEM after mock treatment (left) or mock vs UVP treatment (right panels) for each genotype context; p-values are from two-way ANOVA comparison. (**E**) Flow cytometry analysis of tumors seven days after mock or UVP from wt or B cell k/o mice immunized

and treated as in A; mean+SEM is shown and asterisks denote two-tailed tukey's post hoc test $p<0.05$. (**E**, top) $CD4^+$ T cells from spleens of mice immunized with Tet (control) or polio as in Figure 2A were adoptively transferred to naïve B16 tumor-bearing recipients 1 day prior to intratumoral treatment with DMEM or mRIPO. (**E**, bottom) Mean tumor volume + SEM for mock or mRIPO treated mice for each $CD4^+$ T cell transfer condition; p-values are from two-way ANOVA comparison to the control group. See Figure S6 for a related repeat data set.

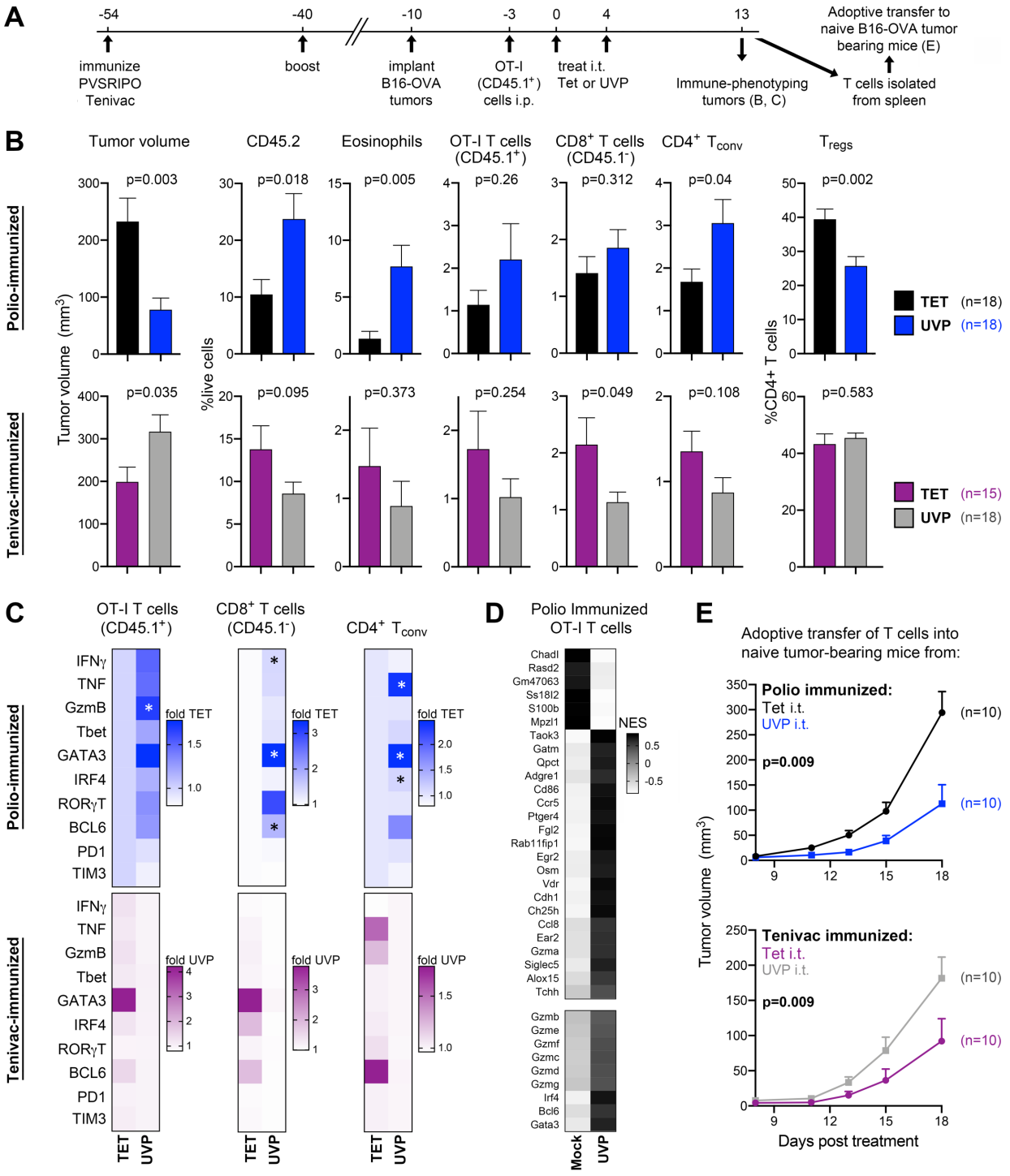

Figure 5. Intratumor recall antigen therapy potentiates antitumor CD8$^+$ T cell function. (**A**) Mice immunized against polio (PVSRIPO) or Tet (Tenivac) were implanted with B16-OVA tumors, followed by adoptive transfer of ex vivo activated OT-I (CD45.1$^+$) cells, and treatment with either Tet or UVP. Thirteen days after treatment tumors and spleens were harvested for analyses in (**B-D**). (**B**) Tumor volume and flow

cytometry analysis from mice treated as in (A). (**C**) Analysis of TIL subsets (OT-I, endogenous $CD8^+$, and conventional $CD4^+$ T cells) for markers of activation and differentiation; gating for OT-I cells is presented in Figure S7. (**D**) Tumor infiltrating OT-I T cells were isolated from polio immunized mice treated with either mock or UVP as in Fig 4A 12 days after treatment. RNA was isolated from CD45.1+ enriched OT-I T cells (see Fig S8A for validation) and analyzed by RNA sequencing. Center and scaled mean enrichment scores are shown for genes that were significantly enriched or depleted in two independent experiments (top panel) or for granzymes, IRF4, BCL6, and GATA3 (bottom panel); n=4 replicates/group. Fig S8B-C presents False Discovery Rate corrected p-values, sample-level enrichment scores from 2 independent experiments, and annotation of relevance of significantly enriched/depleted transcripts. (**E**) Tumor progression in naïve mice upon adoptive transfer of T cells from spleens of mice from experiment in A-C. Mean tumor volume + SEM is shown; p-value is from two-way ANOVA. All data bars represent mean + SEM; heatmaps in (C) were normalized by fold average of the mismatched antigen control; symbols indicate significant Tukey's post-hoc test relative to all other groups (#) or respective DMEM control (*). (A-C) represents pooled results from two independent experiments, data in (E) were repeated twice and a representative series is shown.

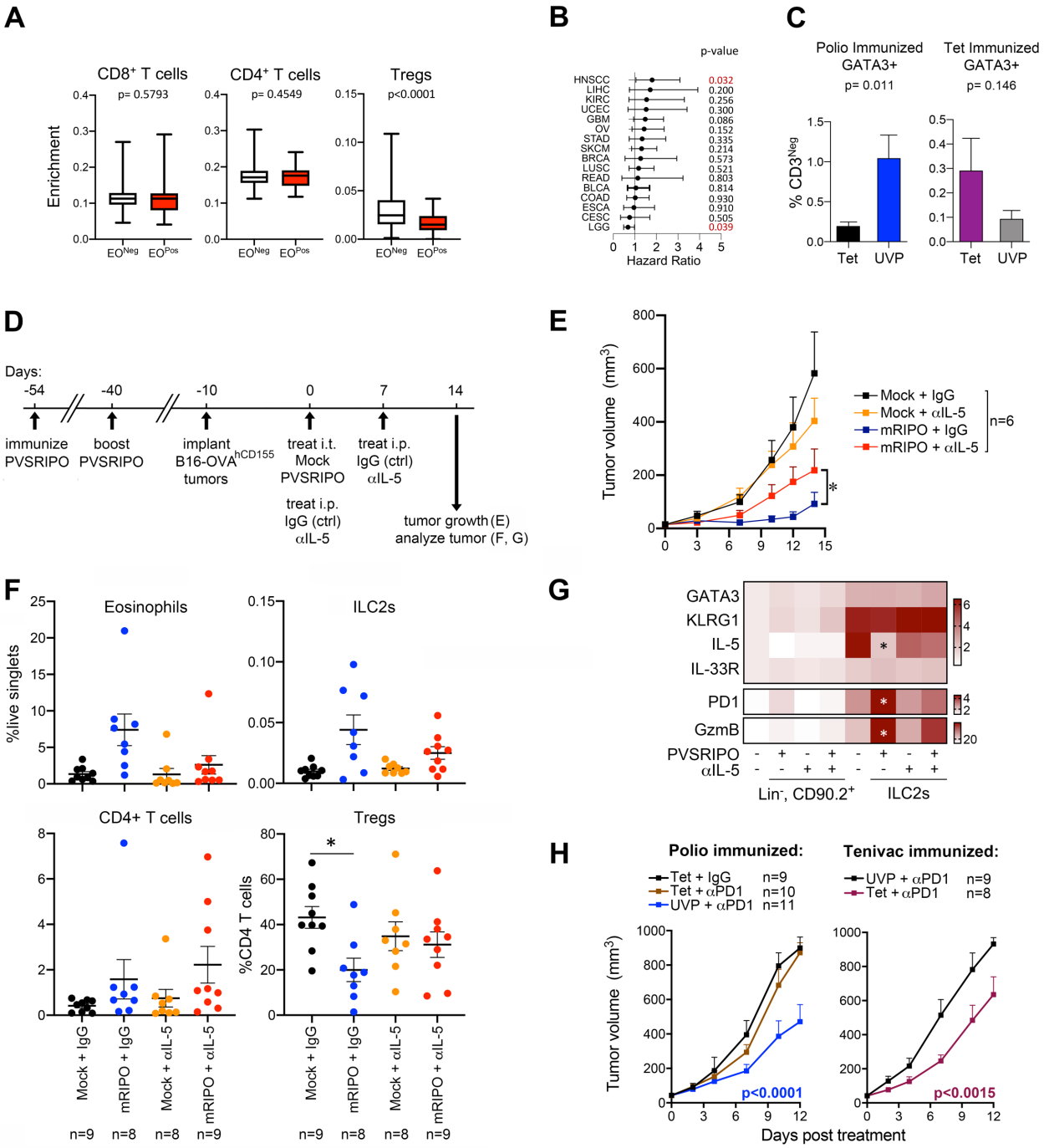

Figure 6. Eosinophils inversely associate with Tregs in human tumors; mRIPO induces antitumor antitumor type II immunity in polio immunized mice. (**A**) Enrichment scores of $CD8^+$ T cells, $CD4^+$ T cells, or Tregs in 29 different cancer types, p-values are from paired t-test. (**B**) Hazard ratios -/+ 95% confidence intervals for denoted cancer types; cancer types with less than 20 deaths in the cohort were

excluded for these analyses; p-value is from Mantel-Cox log-rank test. (**C**) Percentage of GATA3+ $CD3^{Neg}$ cells re-gated from flow cytometry data set presented in Fig 5C, p-values are from unpaired t-test. (**D**) Design for (E-H): hCD155-transgenic mice were vaccinated against polio, implanted with B16-OVA^{hCD155} tumors, and treated with intratumor mock or PVSRIPO in the presence or absence of eosinophil depletion (anti-IL-5 antibody or IgG control, 1mg administered once weekly). Mean tumor volume + SEM (**E**), eosinophil and ILC2 density in tumors (**F**), and phenotype of tumor infiltrating ILC2s ($lineage^{Neg}$, $CD90^{+}$, $CD127^{+}$, $CD25^{+}$) vs lineage negative $CD90^{+}$ cells for comparison are shown (**G**). (**H**) Polio or tetanus immunized mice were treated i.t. with Tet or UVP with control IgG (250μg/mouse every 3 days) or in combination with anti-PD1 antibody (250μg/mouse every 3 days); mean tumor volume + SEM is shown. (**E**) Asterisk indicates Two-way ANOVA $p<0.05$ (two-tailed); (**F-G**) asterisk indicates Tukey's post hoc test $p<0.05$ relative to mock + IgG control; (**H**) p-values are from two-way ANOVA $p<0.05$ compared to recall antigen control. Figs S9-S11 presents gating strategy and extended data.

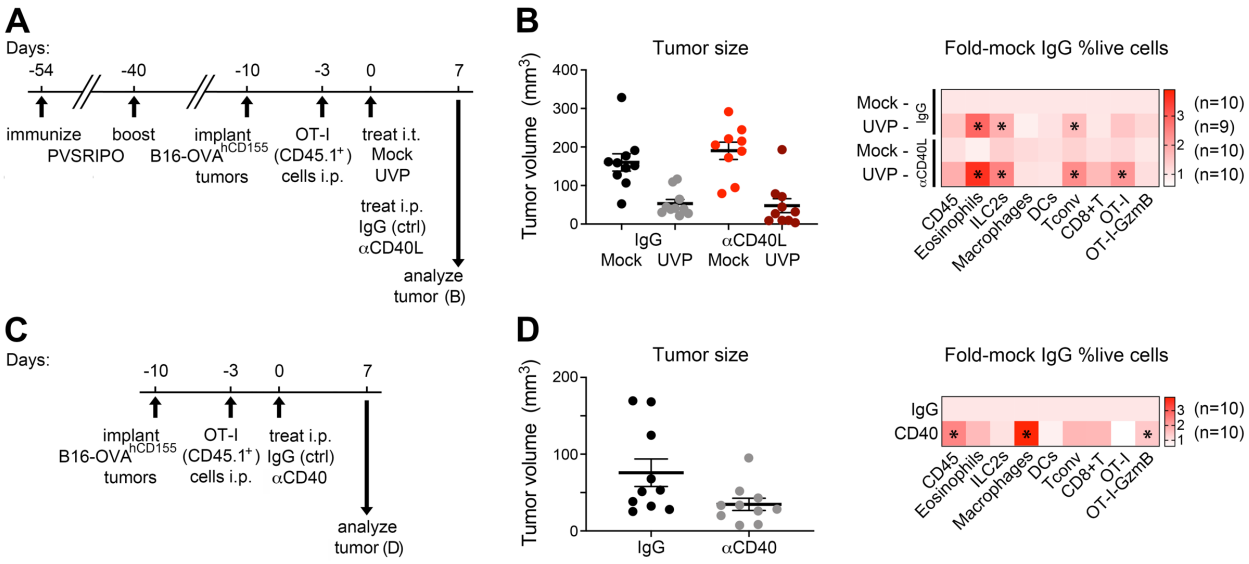

Figure 7. The antitumor efficacy of recall antigens is independent of CD40L-CD40 signaling. (**A**) B16-OVA tumor bearing mice previously immunized against polio received adoptive transfer of OT-I T cells followed by intratumor treatment with either mock or UVP concomitant with control IgG or a CD40L blocking antibody (250μg, every 3 days) for experiment shown in (B). (**B**) Tumor volume (left) and analysis of tumor infiltrating immune cells (right) was conducted 7 days after treatment. Data bars depict mean -/+ SEM; heatmap depicts fold-mock IgG control. (**C**) B16-OVA tumor bearing mice received adoptive transfer of OT-I cells followed by intraperitoneal treatment with control IgG or anti-CD40 antibody (50μg/mouse, once) for experiment shown in (D). (**D**) Tumor volume (left) and analysis of tumor infiltrating immune cells (right) were measured 7 days after treatment. Data bars depict mean -/+ SEM; heatmap depicts fold-mock IgG control. Asterisks indicate Dunnett's post-hoc test relative to mock + IgG control (**B**), or unpaired t test relative to IgG control (**D**). All experiments were repeated at least twice and representative series are shown.